# Electrical and Mechanical Properties of Carbon Nanotube-Epoxy Nanocomposites

**Piyush R. Thakre, Yordanos Bisrat,* Dimitris C. Lagoudas**

*Department of Aerospace Engineering, Materials Science and Engineering Program, Texas A&M University, College Station, Texas 77843-3141*

Received 21 May 2008; accepted 4 July 2009
DOI 10.1002/app.31122
Published online 1 December 2009 in Wiley InterScience (www.interscience.wiley.com).

**ABSTRACT:** In this work, electrical conductivity and thermo-mechanical properties have been measured for carbon nanotube reinforced epoxy matrix composites. These nanocomposites consisted of two types of nanofillers, single walled carbon nanotubes (SW-CNT) and electrical grade carbon nanotubes (XD-CNT). The influence of the type of nanotubes and their corresponding loading weight fraction on the microstructure and the resulting electrical and mechanical properties of the nanocomposites have been investigated. The electrical conductivity of the nanocomposites showed a significantly high, about seven orders of magnitude, improvement at very low loading weight fractions of nanotubes in both types of nanocomposites. The percolation threshold in nanocomposites with SW-CNT fillers was found to be around 0.015 wt % and that with XD-CNT fillers around 0.0225 wt %. Transmission optical microscopy of the nanocomposites revealed some differences in the microstructure of the two types of nanocomposites which can be related to the variation in the percolation thresholds of these nanocomposites. The mechanical properties (storage modulus and loss modulus) and the glass transition temperature have not been compromised with the addition of fillers compared with significant enhancement of electrical properties. The main significance of these results is that XD-CNTs can be used as a cost effective nanofiller for electrical applications of epoxy based nanocomposites at a fraction of SW-CNT cost. © 2009 Wiley Periodicals, Inc. J Appl Polym Sci 116: 191–202, 2010

**Key words:** nanocomposites; conducting polymers; mechanical properties; carbon nanotubes; microstructure-property relationship; electrical conductivity

## INTRODUCTION

There is a growing demand for low cost materials in the microelectronic devices industry,[1] and as a result there is significant research going on in the polymer based nanocomposites for a wide range of properties such as electrical, thermal, mechanical, and magnetic properties.[2-8] What makes the polymers attractive host material is their light weight, the fracture toughness and the tensile strength. In addition, one can easily modify the physical properties of the polymer by using fillers and still keep some of the excellent inherent properties. For example, the conducting polymer composites are made by the addition of conductive fillers into an insulating polymer matrix. Introduction of fillers such as carbon black and iron powder has long been pursued by researchers to modify the electrical properties of the polymers.[9,10] However, such fillers tend to degrade the modulus, the strength, and the glass transition temperature of the nanocomposites. One of the promising filler material is considered to be the carbon nanotubes (CNT)s since they provide good thermal and electrical properties at low loadings compared with carbon black or other metallic reinforcements.[11,12]

The effect of the aspect ratio, the aggregate size, and the dispersion process as a result of functionalization has been reported to affect the percolation limits of nanocomposites.[11-24] Gojny et al.[11] experimentally found that the aspect ratio of the filler, its dispersibility and the ability to agglomerate are crucial parameters for the realization of conductive response at low filler contents and that an increase in the aspect ratio leads to a lower percolation threshold. Li et al.[16] reported similar observation that higher aspect ratio leads to a lower percolation threshold and also developed an analytical model based on interparticle distance concept to explain the effect of dispersion state and aspect ratio of nanotubes on the percolation threshold. Seidel and Lagoudas[22] modeled percolation threshold and effective conductivity using micromechanics and reported that lower aspect ratio for multiwall CNT (MW-CNT) leads to higher

**Present address:* Materials Characterization Facility, Texas A&M University, College Station, Texas 77843.
*Correspondence to:* D. C. Lagoudas (lagoudas@aero.tamu.edu).

Contract grant sponsor: Texas Institute for Intelligent Bio-Nano Materials and Structures for Aerospace Vehicles (NASA); contract grant number: NCC-1-02038.
Contract grant sponsor: the National Science Foundation-Sandia; contract grant number: NSF-DMI-0626460.

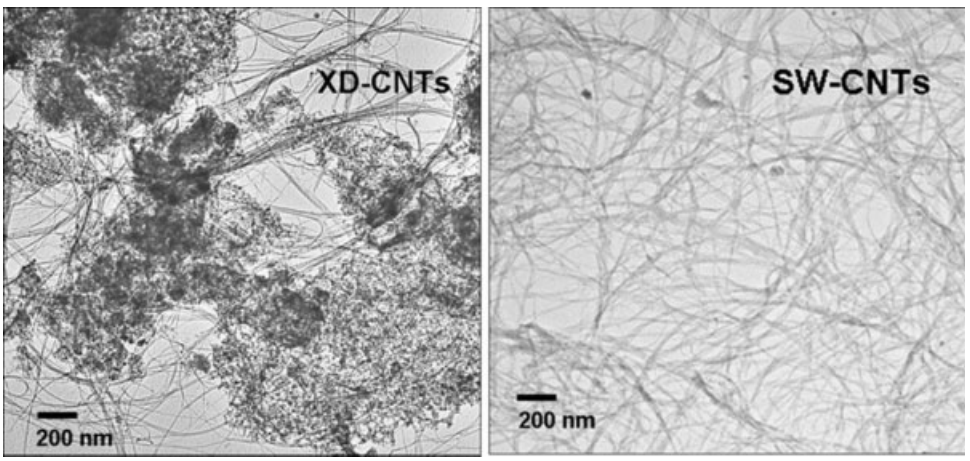


**Figure 1** Transmission electron microscopy images of XD-CNTs and SW-CNTs.

percolation threshold while higher aspect ratio for single walled CNT (SW-CNT) leads to lower percolation threshold. It was also reported that about an order of magnitude increase in aspect ratio results in large increase in effective conductivity of the nanocomposites after percolation. Improvement in dispersion of nanotubes in polymer matrix has been reported to improve electrical and mechanical properties of the nanocomposites.[13,14,15,17,20] Aggregation of nanotubes due to van der Waals interactions and shear forces during mixing has been reported to cause a drop in electrical conductivity.[11,21,23] Sandler et al.[25] reported ultra-low electrical percolation threshold of about 0.005 wt % for epoxy matrix nanocomposites with CVD grown aligned MW-CNTs. The electrical conductivity of the nanocomposites with aligned MW-CNTs was found to be an order of magnitude lower than that with entangled MW-CNTs. Owing to high aspect ratio and good dispersion, nanotubes can reach conductivity thresholds at lower loading levels and can create networks that facilitate electron transport.

In addition to the aspect ratio and the dispersion, several studies have shown that various processing parameters affect the properties of the resulting nanocomposites.[14,15,16,18,26-29] Martin et al. in 2004[18] reported the effect of stirring rates, shear forces and curing temperatures on epoxy matrix nanocomposites with 0.01 wt % of CVD grown MW-CNTs. They suggested high stirring rates and shear forces for separating nanotubes in the initial phase and then, after adding hardener, use of high curing temperatures to enhance the mobility of nanotubes resulting in a better network formation of nanotubes.

The process of covalent and noncovalent functionalization has been suggested as one of the options for better dispersion of nanotubes.[11,16,30-34] Covalent functionalization using silane has been reported to give good dispersion by Thakre et al.,[32] without significant effect on the mechanical properties. The chemical modification of the nanotube surface through covalent functionalization results in reduction of the aspect ratio along with the formation of $sp^3$ carbons on nanotube surface, which decreases the electrical conductivity of the nanotubes.[11,16,32] Therefore, as-received nanotubes have been used in this research without any functionalization, as this work is focused on the electrical properties.

As seen from the literature, the electrical conductivity has been significantly improved by addition of nanotubes and very low electrical percolation limits have been reported for nanocomposites with single walled and multi-walled nanotubes.[2-5,7,11,13-18,12,20,21,25,35-46] However, the cost comparison with cheaper reinforcement particulates does not proportionately favor the use of nanotubes.

The electrical grade CNT (XD-CNT) ,(~ $50 per gram) produced by a high yield process is much cheaper than SW-CNT (~ $350–$1000 per gram); however, the difference in mechanical and electrical properties of nanocomposites consisting of these nanofillers is not known. Thus, the purpose of this article is to examine the electrical and the mechanical properties of XD-CNT and SW-CNT filled epoxy matrix nanocomposites. Section 2 below describes the materials, the nanocomposites preparation and the details of the characterization methods. Results from electrical conductivity measurements and mechanical tests along with transmission optical microscopy and scanning electron microscopy for studying dispersion are presented in Section 3, followed by discussion in Section 4 and conclusions.

## EXPERIMENTAL PROCEDURE

### Materials

Conductive grade XD-CNTs and HiPCO processed SW-CNTs were obtained from Carbon Nanotechnology

Inc. (now Unidym), Houston, Texas[47] and Rice University. The XD-CNTs consisted of a mixture of single walled, double-walled, and multi-walled nanotubes along with carbon black and metallic impurities,[47,48] as shown in the transmission electron microscopy image of typical XD-CNTs in Figure 1. The SW-CNTs consists of bundles of nanotubes (individual SW-CNT diameter 1–1.4 nm[47]). The epoxy resin used was EPON 862 along with aromatic diamine curing agent Epicure W, purchased from Resolution Performance Products.

### Nanocomposite preparation

The nanocomposite samples were prepared using a cast molding method. Three weight percents (0.015 wt %, 0.0225 wt %, and 0.03 wt %) of SW- and XD-CNTs were used to make nanocomposites, labeled hereafter as the epoxy/SW and the epoxy/XD nanocomposites, respectively. The nanotubes were dispersed in a mixture of solvents (ethanol-20 mL and toluene-15 mL) for 1 hour in an ultrasonicator bath (50 kHz). Epoxy resin was then added to nanotube-solvent solution and subjected to magnetic stirring on a hot plate (at about 60°C), until most of the solvent had evaporated. The time required for solvent evaporation was about 30 min under full vacuum. Epicure W curing agent was added to the solvent free epoxy-nanotube mixture at a proportion of 100 : 26.4 by weight. Further mixing was performed manually, followed by magnetic stirring. The mixture was degassed for removing air bubbles until the solution stops showing any bubbles, and this process required variable time based on viscosity of solution. Degassing was followed by casting into a custom-made mold, made out of aluminum.

A two step curing procedure was used with initial temperature set at 121°C for 2 h. followed by 175°C for another 2 h. The samples were left in the oven for a few hours after the curing cycle for post curing with gradual decrease of temperature. A control epoxy specimen was processed using the same method, and solvent was added to the neat resin without any CNTs to investigate the effect of addition and evaporation of the solvent on the electrical conductivity, storage modulus, and glass transition temperature of the control epoxy panel. Specimens were cut from the different sections of each nanocomposite panel. Rectangular specimens ($30 \times 8 \times 2$ $mm^3$) were cut for the dynamic mechanical testing, and square specimens ($20 \times 20$ $mm^2$) were cut for the electrical conductivity measurements. The top and the bottom faces were polished with 600 SiC paper and a thin layer ($\sim$ 100 nm) of silver was deposited by metal evaporation on each face to be used as electrodes. Transmission optical microscopy was performed on the square specimens used for electrical measurements, before the silver electrode deposition. Scanning electron microscopy was performed on fracture surfaces, which were obtained by cracking cooled specimens using nitrogen gas.

### Nanocomposite characterization

Electrical conductivity (AC) measurements were performed using Novo-Control Broadband Dielectric spectrometer at room temperature with voltage amplitude of 1.0 V over a frequency range from 0.01 Hz to 10 MHz. Dynamic Mechanical Analyser (RSA-3, TA Instruments) with a three-point bend module was used to measure the storage and the loss modulus at a constant frequency of 1 Hz. The temperature was ramped up to 200°C from the room temperature, at a constant temperature ramp rate of 2°C/min. A ratio of the storage and the loss modulus, given as tan $\delta$, provided information on the glass transition temperature. For both types of characterization (electrical conductivity and mechanical), at least three samples were tested for each nanocomposite, and an average is reported along with standard deviation. Transmission optical microscopy (TOM) was performed using the Nikon Stereo Photomicroscope and Scanning electron microscopy (SEM) was performed using the JSM-7500F cold emission microscope to characterize the microstructure of the nanocomposites, to elucidate the relationship between the resulting properties and the types and loading levels of the CNTs.

## RESULTS

### Electrical conductivity

An electrically nonconductive polymer matrix can be made conductive by the formation of conductive pathways of filler particles, when the filler content exceeds a critical volume fraction, known as the percolation threshold. The percolation threshold is characterized by a sharp rise in the electrical conductivity as a function of the volume fraction (or weight fraction) of the filler particle content for low frequencies which is identified from frequency independent response of electrical conductivity using AC measurements.

The electrical conductivity measurement as a function of frequency has been shown in Figures 2 and 3, for XD- and SW-CNTs, respectively. For low CNT loadings (less than 0.0225 wt % for XD-CNTs) the conductivity is frequency dependent, i.e., it increases with increasing frequency similar to that of the neat epoxy and the control epoxy. It should be noted that the control epoxy sample showed similar frequency dependence to the neat epoxy, indicating that the addition of the solvents during the processing did not affect the epoxy electrical conductivity. In the

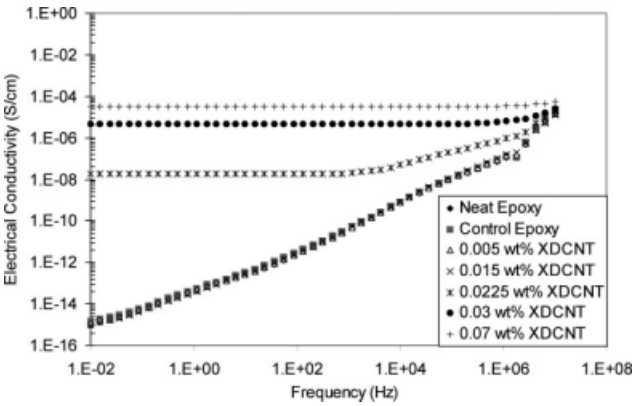


**Figure 2** Log-log plot of electrical conductivity of the epoxy/XD nanocomposites as a function of frequency for various loading weight fractions of XD-CNTs.

vicinity and above the percolation threshold (0.0225 wt % for epoxy/XD and 0.015 wt % for epoxy/SW) the conductivity becomes frequency independent. The AC measurements allow measuring electrical conductivity as a function of frequency. The insulating (or nonpercolated) specimens show frequency dependent response. As soon as conductive networks form in the nonconducting material, such a transition from nonconductive to conductive material, is represented by frequency independent response. There can be frequency dependent response at higher frequencies for not fully percolated specimens. In relation to the neat and the control epoxy, there was about seven to eight orders of magnitude increase in the conductivity at 0.01 Hz for epoxy/XD- and epoxy/SW nanocomposites. Above the percolation threshold, the conductivity continues to increase but only marginally, i.e., about two orders of magnitude for epoxy/XD nanocomposites (0.03 wt %) and about one order of magnitude for epoxy/SW nanocomposites (0.03 wt %).

To compare the electrical conductivities of epoxy/XD and epoxy/SW nanocomposites as a function of weight fraction of nanotubes, Figure 4 has been plotted using electrical conductivity data from Figures 2 and 3 at low frequency of 0.01 Hz. The scatter in data has been plotted in Figure 4; however, the error bars are overlapped by the size of each data point. The difference in percolation thresholds can be observed in both nanocomposites from the semi-log plots. For epoxy/SW nanocomposites, percolation occurs at a lower weight fraction (0.015 wt %) than that for epoxy/XD nanocomposites (0.0225 wt %) and corresponding frequency independence is confirmed from Figures 2 and 3. The vertical dotted lines in Figure 4 points to various weight fractions of XD- and SW-CNTs. Postpercolation increase for epoxy/SW nanocomposites has been observed to be from about 1E-7 S/cm for 0.0225 wt % to about 1E-6 S/cm for 0.03 wt % of SW-CNTs, while for epoxy/XD nanocomposites, from about 1E-7 S/cm for 0.0225 wt % to about 1E-5 S/cm for 0.03 wt % of XD-CNTs. Additional data points corresponding to XD-CNTs weight fraction of 0.07 wt % and 0.15 wt %, and 0.07 wt % for SW-CNTs have been plotted in Figure 4 to show that the increase in conductivity becomes smaller after certain weight fraction, as indicated by the plateau in the conductivity curve after percolation. Frequency dependence of conductivity of nanocomposites is sensitive to corresponding microstructure formation of conducting networks and can be related to the percolation state of the nanofillers within the nanocomposite.

## Transmission optical microscopy

The difference in percolation thresholds and the effects of higher loading of nanotubes for these nanocomposites can be related to the formation of microstructure as a result of differences in the types of nanotubes. Figure 5 compares the microstructures of the epoxy/SW and epoxy/XD nanocomposites at

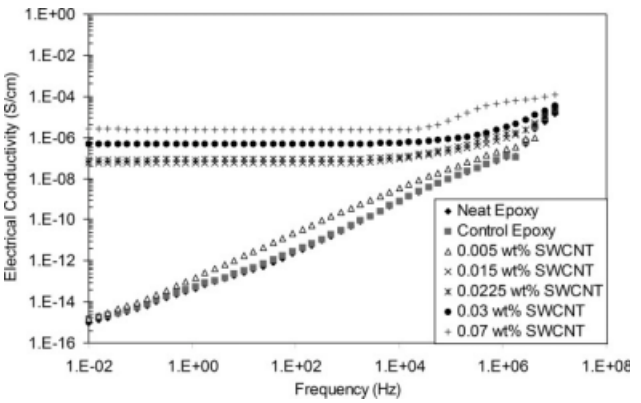


**Figure 3** Log-log plot of electrical conductivity of the epoxy/SW nanocomposites as a function of frequency for various loading weight fractions of SW-CNTs.

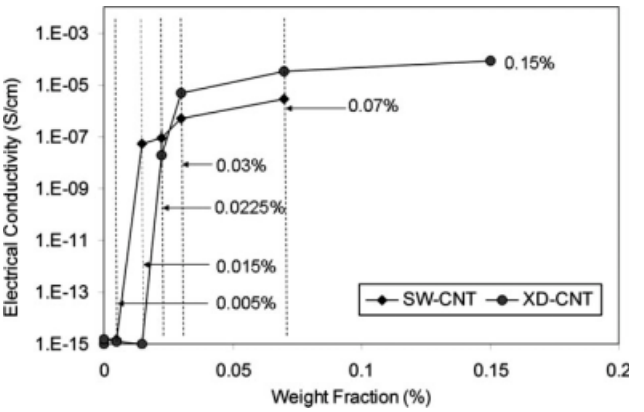


**Figure 4** Semi-log plot of electrical conductivity as a function of loading weight fractions of CNTs for epoxy/XD and epoxy/SW nanocomposites.

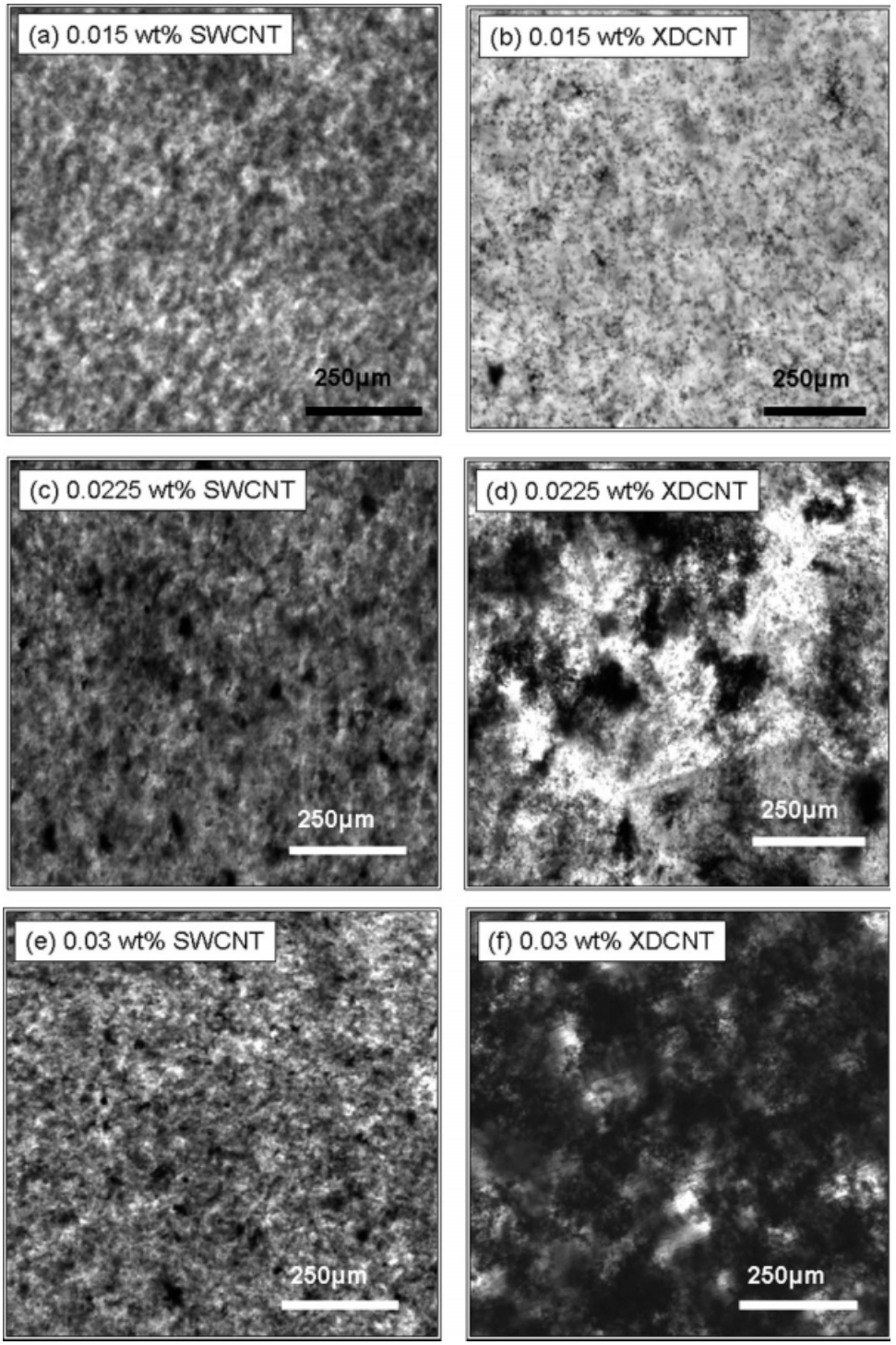


**Figure 5** Transmission optical microscopy images of epoxy/SW and epoxy/XD nanocomposites for different weight fractions of CNTs.

various CNT loading levels. The darker regions in the TOM micrographs represent the presence of nanotube bundles and the lighter regions represent the surrounding epoxy matrix. Figure 5(a,c,e) shows the dispersion of SW nanotube bundles in epoxy/SW nanocomposites and Figure 5(b,d,f) shows the dispersion of XD nanotubes in epoxy/XD nanocomposites. As it can be seen, the formation of microstructure and percolating networks is indeed different for the same weight percents of XD- and SW-CNTs. As the weight fraction of CNTs is increased for epoxy/XD nanocomposites, the nanotubes tend to form bigger clusters, unlike in epoxy/SW nanocomposites.

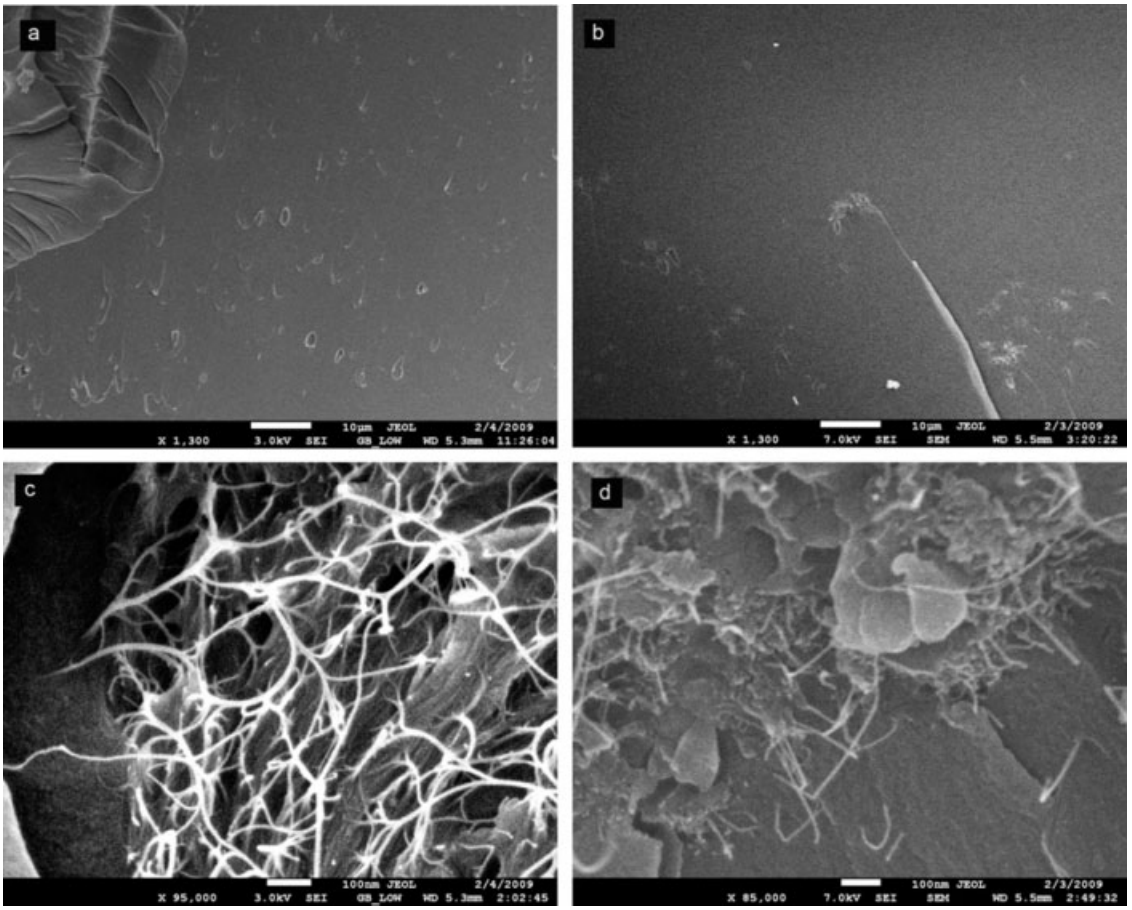


**Figure 6** Scanning electron microscopy images of epoxy/SW and epoxy/XD nanocomposites at low magnification (a,b) and high magnification (c,d).

Figure 5 shows that the amount of agglomeration with increased loading weight fraction is higher in epoxy/XD nanocomposites (b,d,f), than in epoxy/SW nanocomposites (a,c,e). The micrograph in Figure 5(f) is seen to be almost opaque due to big agglomerates formed by XD-CNTs.

### Scanning electron microscopy

SEM studies on fracture surfaces were performed to study the morphological differences in the epoxy/XD and epoxy/SW nanocomposites.

As seen from Figure 6(a,b), the SW-CNTs are more homogeneously distributed as compared with XD-CNTs for 0.03 wt % specimens. Similar observations were made in Figure 5, i.e., XD-CNTs tends to agglomerate more with increasing weight fractions, resulting in lesser degree of homogeneity compared with SW-CNTs. Figure 6(c,d) represents images at higher magnification to study the network formation and aspect ratio of the nanotubes. Figure 6(c) for epoxy/SW nanocomposite shows longer length nanotube bundles (higher aspect ratio) as compared with Figure 6(d) for epoxy/XD nanocomposites. Also a homogeneous SW-CNT network formation is visible in Figure 6(c) as compared with agglomeration of XD-CNTs and possibly presence of some impurities in Figure 6(d).

### Dynamic mechanical analysis

Dynamic mechanical analysis (DMA) measurements were performed to find the storage modulus ($E'$), the loss modulus ($E''$) and the glass transition temperature (Tg), and the results are summarized for neat

**TABLE I**
**DMA Measurements for Epoxy/SW and Epoxy/XD Nanocomposites ($E'$ and $E''$ Reported at 30°C)**

| | $E'$ (GPa) | $E''$ (MPa) | Tg (°C) |
|---|---|---|---|
| Epoxy | 2.8 ± 0.3 | 91.6 ± 12.3 | 129 ± 0.1 |
| Epoxy/SW nanocomposites | | | |
| 0.015 wt % | 2.5 ± 0.1 | 101.6 ± 22.1 | 141 ± 1.2 |
| 0.0225 wt % | 2.7 ± 0.1 | 110.0 ± 23.2 | 148 ± 2.0 |
| 0.03 wt % | 2.9 ± 0.4 | 131.5 ± 21.5 | 149 ± 1.6 |
| Epoxy/XD nanocomposites | | | |
| 0.015 wt % | 3.0 ± 0.1 | 173.4 ± 9.3 | 140 ± 7.0 |
| 0.0225 wt % | 2.8 ± 0.2 | 117.9 ± 7.0 | 149 ± 1.0 |
| 0.03 wt % | 3.3 ± 0.2 | 175.1 ± 65.4 | 133 ± 1.4 |

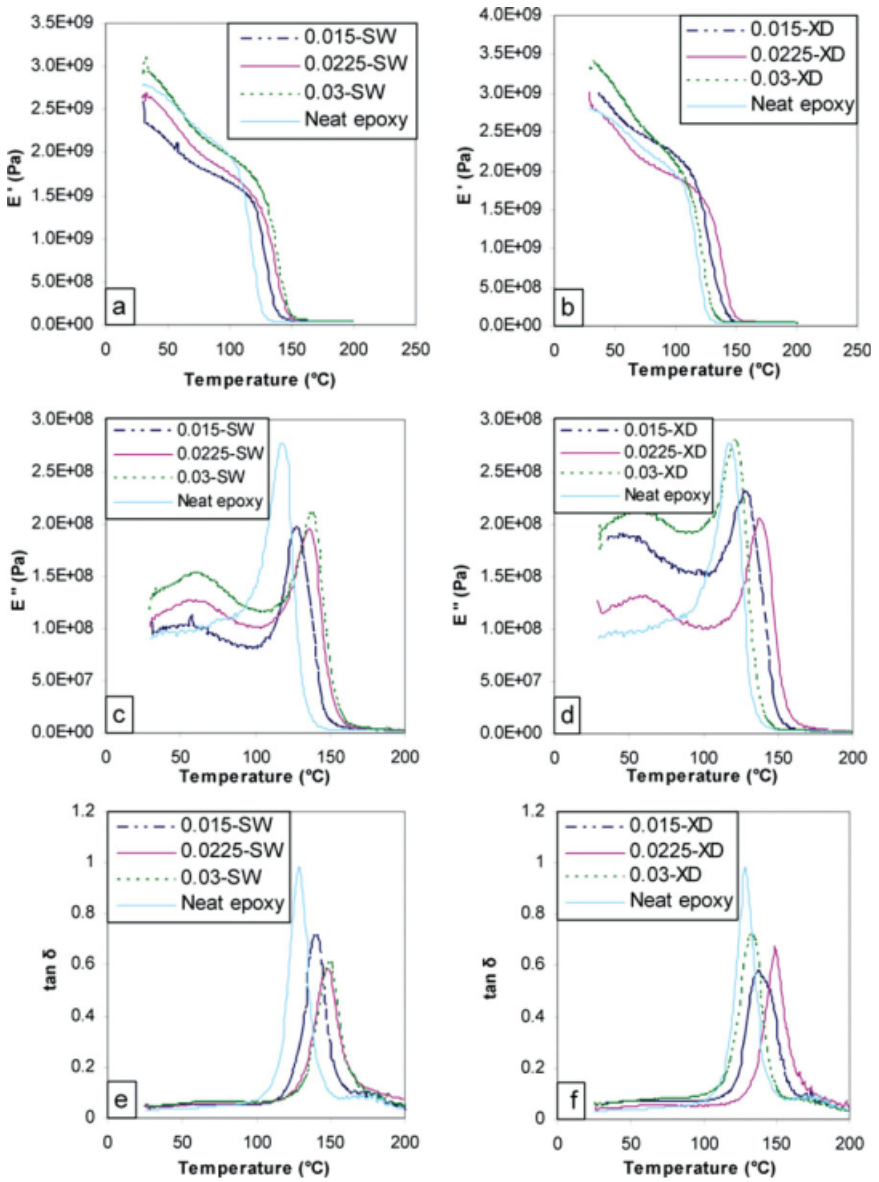


**Figure 7** DMA results for epoxy/SW and epoxy/XD nanocomposites. [Color figure can be viewed in the online issue, which is available at www.interscience.wiley.com.]

epoxy, epoxy/SW, and epoxy/XD nanocomposites in Table I.

CNT have been reported to improve the mechanical properties of nanocomposites,[6,13,26,32-34,41,49] however, the reported weight or volume fractions were much higher (50–100 times) than the ones used in this study. For such extremely low weight fractions of nanotubes used in our study, minimal change is expected in the mechanical properties. The storage modulus and loss modulus values are reported in Table I for measurements at 30°C, whereas the modulus values during complete temperature sweep, starting from room temperature to well above glass transition, is shown in Figure 7. The effect of different weight fractions of SW and XD nanotubes on the storage modulus, $E'$ [Fig. 7(a,b)], and the loss modulus, $E''$ [Fig. 7c,d)], and the tan δ curves (glass transition temperatures, Tg is measured corresponding to the peak), [Fig. 7(e,f)] and comparison with neat epoxy is shown in Figure 7. The storage modulus does not show any significant improvement or degradation as compared with neat epoxy for epoxy/SW as well as epoxy/XD nanocomposites and lies within the scatter observed from standard deviations.

Higher weight fractions have not been reported in this work, as the focus of this article is on the percolation thresholds and the postpercolation behavior of the electrical conductivity and its correlation to morphology of dispersed nanotubes. However, the loss modulus and the glass transition temperature measured from the DMA test can give some information about the dispersion state of the nanotubes

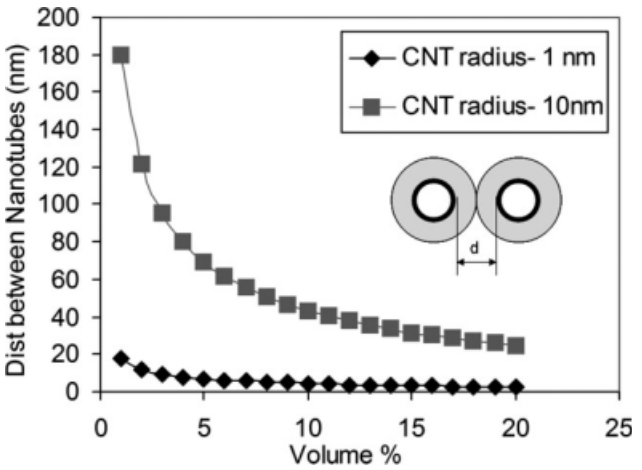


**Figure 8** Change in the distance between nanotubes surfaces, d, as a function of change in nanotube volume percent for two different nanotube diameters in an ideal case study.

throughout the specimen and the effect of localized dispersion state on the overall transition behavior from glassy to rubbery state. The changes in loss modulus are related to the changes in energy dissipation mechanisms, and the change in glass transition temperature is related to the mobility of polymeric chains during the transition from glassy to rubbery state.

As seen from Figure 7(a) and Table I, the storage modulus for epoxy/SW nanocomposites is comparable to the neat epoxy modulus and lies within the standard deviation. However, the storage modulus for epoxy/XD nanocomposites seems to be slightly increased, especially for 0.03 wt % XD-CNTs.

The loss modulus values at room temperature showed an increase for epoxy/SW as well as for epoxy/XD nanocomposites, as shown in Figure 7(c,d). The increase in loss modulus is prominent for all specimens, even after accounting for the scatter in the standard deviations. These shifts are likely to be due to the increased energy dissipation in the form of heat as a result of nanotube-nanotube friction. Energy dissipation due to crack initiation or crack growth does not seem possible, because extremely small load was applied during the DMA tests. As seen from Figures 5 and 6, SW as well as XD nanotubes exist in the form of bundles and friction between nanotubes seems to be a plausible reason for an increase in energy dissipation at room temperature, leading to an increase in loss modulus.

Figure 7(e) shows that the glass transition temperatures increased by about 10°C for 0.015 wt % and about 17 to 20°C for 0.0225 and 0.03 wt % SW-CNTs, respectively, as compared with neat epoxy. The Tg increase for epoxy/XD nanocomposites [Fig. 7(f)] was about 10°C for 0.015 wt % and about 20°C for 0.0225 wt %, but insignificant change of about 3°C for 0.03 wt % XD-CNTs as compared with the neat epoxy. The increase in Tg for such small weight fractions seems to be related to the localized dispersion state of nanotubes in epoxy matrix. Polymeric chains start moving during the transition process from glassy to rubbery state. The presence of nanotube bundles, as seen from Figures 5 and 6, act as a hurdle for movement of molecular chains of polymer at temperatures near Tg, which in turn leads to an increase in the glass transition temperature.

## DISCUSSION

There are several parameters, like dispersion state, aspect ratio, processing method, aggregate size, presence of impurities, and ratio of metallic-semiconducting nanotubes, etc., that affect the percolation threshold and the postpercolation electrical conductivity. The effect of aspect ratio, interparticle distance between nanotubes and nanotube agglomeration is discussed in the following sections. In addition, the experimental percolation thresholds have been compared with the theoretical percolation thresholds for the nanocomposites obtained from a power law model.

### Effect of aspect ratio and distance between nanotubes

Nanotubes tend to agglomerate due to van der Waals interactions, particularly in absence of any surface modification through chemical functionalization. As a result of bundling, the conductive inclusions have a larger effective diameter which yields a reduced aspect ratio. Thus, increased weight/volume fraction of nanotubes is required to achieve the percolation. As seen from SEM images in Figure 6(c,d), the aspect ratios of nanotube bundles for XD-CNTs are seen to be smaller as compared with the aspect ratios of SW-CNT bundles. Due to the presence of larger diameter MW-CNTs in the bundle formation of XD-CNTs, it is expected that the conductive inclusions of XD-CNTs will have a larger effective diameter as compared with conductive inclusions of SW-CNT bundles. The outcome is the reduction of the effective aspect ratio for XD-CNT bundles, as observed from Figure 6. The lower percolation threshold for epoxy/SW nanocomposites compared with that with epoxy/XD nanocomposites indicates an agreement with Gojny et al.,[11] Seidel and Lagoudas,[22] and Li et al.[16] for comparison between SW and MW-CNTs embedded epoxy matrix nanocomposites.

A simplified approach has been taken for analyzing the electrical conductivity results using two possible differences between SW- and XD-CNTs. Firstly, the change in surface area to volume ratio with

respect to change in nanotube aspect ratios and secondly, the change in the distance between nanotube surfaces surrounded by an epoxy interphase as a function of nanotube diameter and nanotube volume fraction. XD-CNTs consist of a mixture of MW-CNT, SW-CNT, and other carbon/metallic impurities. SW-CNTs are smaller diameter CNTs as compared with MW-CNTs and also SW-CNTs are observed to be usually longer than MW-CNTs. The surface area to volume ratio is a function of radius of the conductive inclusions. For smaller diameter conductive inclusions, the surface area or volume ratio is higher compared with larger diameter conductive inclusions. Thus, the interface area available for charge conduction is higher for smaller diameter conductive inclusions. In the case of smaller diameter (high aspect ratio) SW-CNTs, higher surface area to volume ratio results in greater ability for charge conduction, resulting in lower percolation thresholds. In the case of XD-CNTs, the surface area to volume ratio is smaller due to the presence of MW-CNTs and also due to bigger conductive inclusions formed by agglomeration. Thus, the observation of higher percolation threshold can be inferred qualitatively.

The diameter of nanotubes can also have an effect on the electrical conductivity, as the distance between nanotube surfaces changes in case of an ideal homogeneous dispersion, for the same length and weight fraction of nanotubes. Here, a simplified geometrical approach can be used for a qualitative discussion of the results. The volume fraction can be assumed to be close to the weight fractions used in this study, because of the almost similar densities for the epoxy matrix ($\sim$ 1.2 g/cc) and the nanotubes ($\sim$ 1.3 g/cc). If two different nanotube diameters are considered, e.g., 1 and 10 nm (1 nm representing SW-CNT and 10 nm representing XD-CNT), in an ideal case of well aligned and homogeneously dispersed nanotubes, one can plot the distance between nanotube surfaces as a function of change in volume fraction of nanotubes, as shown in Figure 8. The distance between nanotube surfaces is calculated by approximating a concentric cylinder consisting of a nanotube surrounded by the matrix. The ratio of the radius of the nanotube and the matrix cylinder is proportional to the volume fraction of the nanotube to the matrix material. As seen from Figure 8, for the same volume percent of nanotubes, the distance, $d$, between 1 nm diameter nanotubes is smaller compared with 10 nm diameter nanotubes. Thus, for the same volume percent of nanotubes in a nanocomposite, the distance between nanotubes' surfaces increases with increasing nanotube diameter. So these observations indicates a possibility for easier electron hopping in case of epoxy/SW nanocomposites due to smaller diameter nanotube bundles and thus lower separation between nanotubes, resulting in the lower percolation threshold compared with the epoxy/XD nanocomposites.

Figure 8 represents ideal condition for aligned, homogeneously distributed and well dispersed CNTs. From Figure 8, the separation distance between SW-CNTs is about 18 nm for 1 vol % of SW-CNTs, and for 10 vol % CNTs, the separation distance is about 4 nm. The real nanocomposites have randomly oriented bundles of nanotubes. Also, the local volume fraction can be significantly higher than the global volume fraction of nanotubes due to bundling of nanotubes, in which case the distance between SW-CNTs can be shorter than 18 nm (from Fig. 8). However, the exact distance required for electron hopping is not known, but, it is known that electron hopping is one of the mechanisms for increasing electrical conductivity in the nanocomposite specimens, and present argument shows the effect of nanotube diameter on the distances required for electron hopping. In case of XD-CNTs, the separation distances are much greater, as seen from Figure 8, which indicates bleak possibility for electron hopping mechanism. However, XD-CNTs also contain some proportion of SW-CNTs and thus introducing a possibility for electron hopping mechanism. This will help in reducing the percolation threshold for XD-CNTs reinforced nanocomposites. This provides a possible explanation for small difference in the percolation thresholds between SW-CNTs and XD-CNTs reinforced nanocomposites, as observed from the experimental results in this study.

Seidel and Lagoudas[22] reported the formation of conductive networks as the principle cause for the large increase in effective conductivity for MW-CNTs, whereas both the formation of conductive networks and electron hopping lead to a large increase in conductivity at very low SW-CNT concentrations. The percolation threshold was reported to be lower for SW-CNT as compared to MW-CNT. This experimental results for percolation threshold validates the modeling results from Seidel and Lagoudas.[22] However, due to the presence of SW-CNTs in the mixture of XD-CNTs, the difference in the percolation thresholds between SW-CNT and XD-CNT is not large as compared with modeling results. As seen from TOM micrographs in Figure 5 and SEM micrographs in Figure 6, the conductive network formation with increasing weight fraction of CNTs is more prominent (dense network) in the case of XD-CNTs, as compared with SW-CNTs, due to XD-CNT agglomeration. The dense network of nanotubes brings more nanotubes in direct physical contact, which could be a positive attribute for postpercolation electrical conductivity. This can be interpreted qualitatively, as the main reason for the larger increase in postpercolation electrical conductivity for XD-CNTs, by about two orders of

magnitude for 0.03 wt % XD-CNTs, as compared with one order of magnitude increase for 0.03 wt % SW-CNTs.

### Effect of agglomeration of nanotubes

In case of the MW-CNTs, multiple graphene layers are separated by 0.34 nm with van der Waals interaction between the layers, in addition to the interaction with other surrounding entities. The number of carbon atoms per unit length is more for a MW-CNT as compared with a SW-CNT.

Considering an isolated MW-CNT and a SW-CNT, each carbon atom on a MW-CNT has more number of carbon atoms to interact with surrounding species, i.e., MW-CNTs or SW-CNTs or other carbon impurities, as compared with an atom on a SW-CNT. This leads to higher van der Waals interaction forces between MW-CNT and surrounding species, i.e., MW-CNTs or SW-CNTs or other carbon impurities. Hence, MW-CNTs have a tendency to form bigger agglomerates and as in case of XD-CNTs (which is a cocktail of MW-CNTs, SW-CNTs, and other impurities), the same phenomenon is observed, as can be seen from the Figure 5.

The effect of interaction forces (van der Waals forces) between nanotubes on the percolation threshold has been studied by Grujicic et al.[50] through analytical and numerical modeling. They reported that the interaction between nanotubes due to van der Waals forces increased the percolation threshold as compared with nanotubes without interaction forces. Also it was seen from their numerical model that the nanotubes tended to agglomerate in an attempt to align themselves when interaction forces were introduced between the nanotubes (Fig. 4).[50] The analytical percolation model predicted similar behavior of increased percolation threshold by introduction of interaction forces between nanotubes. The predictions of the model are in good agreement with our experimental observation of higher percolation threshold for epoxy/XD nanocomposites and agglomeration of XD nanotubes.

In addition to higher van der Waals forces between MW-CNTs, the tunneling resistance, as shown by Li et al.[38] for higher diameter nanotubes is lower and the cutoff thickness for tunneling distance is shown to be 1.8 nm. Therefore, MW-CNTs with 0.34 nm distance between inner layers would have comparatively greater electron tunneling as compared with SW-CNTs, thus leading to higher postpercolation conductivity for the nanocomposites. Before percolation, formation of conducting network will govern the percolation threshold value. The XD-CNTs form bigger agglomerates resulting in inhomogeneous distribution through out the specimen and poor physical contact during network formation as compared with corresponding weight fraction of SW-CNTs (as seen from SEM and TOM images). Hence, SW-CNTs are expected to percolate earlier; however, postpercolation conductivity of XD-CNTs is expected to be higher as seen from our results.

### Comparison with theoretical percolation threshold using power law model

The theoretical percolation threshold in composite materials has been given by the following power law model[35,51]:

$$\sigma = \mathrm{A}(V - Vc)^{\mathrm{t}} \tag{1}$$

where $\sigma$ is the electrical conductivity, $V$ is the filler volume fraction, $V_c$ is the critical volume fraction (volume fraction at percolation) and $A$ and $t$ are percolation parameters. The filler volume fraction, $V$, is selected for the conductive nanocomposites and the critical volume fraction, $V_c$, is varied such as to obtain best power law fit. The volume fractions in eq. (1) are replaced with weight fractions used in the experimental study. Since the matrix and the nanotube densities are about the same, the volume fractions and the weight fractions would be almost same. The value for $t$ has been reported from 1.30 to 3.10 as per Ounaies et al.[51] and from 0.87 to 1.79 as per Grujicic et al.[50] The value of $A$ should ideally converge to the electrical conductivity of the nanotubes.[51] However, the value of $A$ is usually found to be much lower than the theoretical electrical conductivity of nanotubes ($\sim$ 1000 S/cm[22]). One of the reasons for lower value for $A$ is due to the presence of contact resistance within the conductive path, i.e., between two adjacent nanotubes, which decreases the effective conductivity of the nanotubes. At low weight percents of nanotubes, a physical contact between nanotubes, which is required to form paths between conductive inclusions in direct contact, is absent. Thus, the value of $A$ is found to be much lower than expected. Power law fitting of the log $\sigma$ versus log ($V$-$V_c$) yielded best fit for 0.0225 wt % of XD-CNTs with fitting parameters, $A$ and $t$, being 7.0E-04 and 1.02, respectively. Ounaies et al.[51] reported values for $A$ of 6.7E-04 and $t$ of 1.38 for their nanocomposites (percolation at 0.5 wt %).

Grujicic et al.[50] presented percolation results for interacting versus noninteracting nanotubes through analytical and numerical modeling. The interaction was considered by the presence of van der Waals forces between the nanotubes. The value of $t$ was reported to be 0.87 and 1.17 for noninteracting and interacting nanotubes, respectively. The corresponding value of $A$ was 1.6E-06 for noninteracting nanotubes and 2E-05 for interacting nanotubes. It seems that the value of fitting parameters, $t$ and $A$,

increases with increasing interaction of nanotubes. The variations in reported $A$ and $t$ values in literature are expected to be due to different processing methods, dispersion state of nanotubes, bundle sizes, and interaction between nanotubes and with impurities. It is estimated by the power law model that the percolation for epoxy/XD nanocomposites occurs around 0.0225 wt %. So the theoretical predictions from the power law model are in good agreement with our experimental results.

The theoretical results for SW-CNTs also showed good agreement with the experimental results. Power law fitting yielded $A$ of 2.6E-03 and $t$ of 2.04 for $V_c$ of 0.016 wt % SW-CNTs. This seemed to be the best fit possible after consideration of a lot of various critical weight fractions. The increased value of $A$ indicates better physical contacts in the formation of conductive network, yielding higher effective conductivity of SW-CNTs as compared to XD-CNTs. An increase in the value of $t$ may represent better interaction between SW-CNTs at low volume fractions as compared with XD-CNTs. The theoretical prediction of percolation threshold for SW-CNTs is in good agreement with experimental observation of percolation threshold, i.e., close to 0.015 wt %, for epoxy/SW nanocomposites.

## CONCLUSIONS

A processing method was developed for preparing nanocomposites containing varying weight fractions of SW-CNTs and XD-CNTs, whose electrical and mechanical properties are investigated in this work. The results are presented with respect to the variation of the microstructure as observed from transmission optical microscopy and scanning electron microscopy. Electrical percolation threshold for epoxy/SW nanocomposites (0.015 wt %) is found to be lower than the percolation threshold for epoxy/XD nanocomposites (0.0225 wt %). The increase in electrical conductivity after percolation is found to be higher for XD-CNTs by an order of magnitude as compared with SW-CNTs at 0.03 wt % of nanotubes. The major enhancement of the electrical conductivity is achieved without compromising the storage modulus with the addition of either SW- or XD-CNTs. The main finding of this work is that a significant improvement in the electrical conductivity has been achieved for both epoxy/SW and epoxy/XD nanocomposites as compared with neat epoxy by about seven to eight orders of magnitude at percolation and about eight to 10 orders of magnitude postpercolation. The improvement for epoxy/XD nanocomposites comes at a much lower cost than epoxy/SW nanocomposites, even after considering additional weight fraction of XD-CNTs due to the differences in the percolation threshold.

Authors would like to acknowledge some useful discussions with Dr. Zoubeida Ounaies and the use of Electroactive Materials Lab with assistance from Mr. S. Banda and Mr. S. Deshmukh. Authors would also like to acknowledge the use of Materials Characterization Facility and Microscopy and Imaging Center at Texas A & M University.

## References

1. Prasher, R. S.; Chang, J.-Y.; Sauciuc, I.; Narasimhan, S.; Chau, D.; Chrysler, G.; Myers, A.; Prstic, S.; Hu, C. Intel Technol J 2005, 9, 285.
2. Dos Santos, A. S.; Leite, T. D. N.; Furtado, C. A.; Welter, C.; Pardini, L. C.; Silva, G. G. J Appl Polym Sci 2008, 108, 979.
3. Zilli, D.; Goyanes, S.; Escobar, M. M.; Chiliotte, C.; Bekeris, V.; Cukierman, A. L.; Rubiolo, G. H. Polym Compos 2007, 28, 612.
4. Thostenson, E. T.; Chou, T. W. Carbon 2006, 44, 3022.
5. Moniruzzaman, M.; Winey, K. I. Macromolecules 2006, 39, 5194.
6. Miyagawa, H.; Misra, M.; Mohanty, A. K. J Nanosci Nanotechnol 2005, 5, 1593.
7. Martin, C. A.; Sandler, J. K. W.; Windle, A. H.; Schwarz, M. K.; Bauhofer, W.; Schulte, K.; Shaffer, M. S. P. Polymer 2005, 46, 877.
8. Biercuk, M. J.; Llaguno, M. C.; Radosavljevic, M.; Hyun, J. K.; Johnson, A. T.; Fischer, J. E. Appl Phys Lett 2002, 80, 2767.
9. Prasse, T.; Flandin, L.; Schulte, K.; Bauhofer, W. Appl Phys Lett 1998, 72, 2903.
10. Prasse, T.; Ivankov, A.; Sandler, J.; Schulte, K.; Bauhofer, W. J Appl Polym Sci 2001, 82, 3381.
11. Gojny, F. H.; Wichmann, M. H. G.; Fiedler, B.; Kinloch, I. A.; Bauhofer, W.; Windle, A. H.; Schulte, K. Polymer 2006, 47, 2036.
12. Moisala, A.; Li, Q.; Kinloch, I. A.; Windle, A. H. Compos Sci Technol 2006, 66, 1285.
13. Bal, S. J Sci Ind Res 2007, 66, 752.
14. Chen, H.; Muthuraman, H.; Stokes, P.; Zou, J. H.; Liu, X.; Wang, J. H.; Huo, Q.; Khondaker, S. I.; Zhai, L. Nanotechnology 2007, 18, 415606-1.
15. Grossiord, N.; Loos, J.; Regev, O.; Koning, C. E. Chem Mater 2006, 18, 1089.
16. Li, J.; Ma, P. C.; Chow, W. S.; To, C. K.; Tang, B. Z.; Kim, J. K. Adv Funct Mater 2007, 17, 3207.
17. Liu, L.; Grunlan, J. C. Adv Funct Mater 2007, 17, 2343.
18. Martin, C. A.; Sandler, J. K. W.; Shaffer, M. S. P.; Schwarz, M. K.; Bauhofer, W.; Schulte, K.; Windle, A. H. Compos Sci Technol 2004, 64, 2309.
19. Miyagawa, H.; Drzal, L. T. Polymer 2004, 45, 5163.
20. Sandler, J.; Shaffer, M. S. P.; Prasse, T.; Bauhofer, W.; Schulte, K.; Windle, A. H. Polymer 1999, 40, 5967.
21. Schmidt, R. H.; Kinloch, I. A.; Burgess, A. N.; Windle, A. H. Langmuir 2007, 23, 5707.
22. Seidel, G. D.; Lagoudas, D. C. J Compos Mater 2009, 43, 917.
23. Bai, J. B.; Allaoui, A. Compos A 2003, 34, 689.
24. Valentini, L.; Puglia, D.; Frulloni, E.; Armentano, I.; Kenny, J. M.; Santucci, S. Compos Sci Technol 2004, 64, 23.
25. Sandler, J. K. W.; Kirk, J. E.; Kinloch, I. A.; Shaffer, M. S. P.; Windle, A. H. Polymer 2003, 44, 5893.
26. Wichmann, M. H. G.; Sumfleth, J.; Fiedler, B.; Gojny, F. H.; Schulte, K. Mech Compos Mater 2006, 42, 395.
27. Lau, K. T.; Lu, M.; Liao, K. Compos Appl Sci Manuf 2006, 37, 1837.
28. Lanticse, L. J.; Tanabe, Y.; Matsui, K.; Kaburagi, Y.; Suda, K.; Hoteida, M.; Endo, M.; Yasuda, E. Carbon 2006, 44, 3078.
29. Pecastaings, G.; Delhaes, P.; Derre, A.; Saadaoui, H.; Carmona, F.; Cui, S. J Nanosci Nanotechnol 2004, 4, 838.
30. Krishnamoorti, R. MRS Bull 2007, 32, 341.

31. Mitchell, C. A.; Bahr, J. L.; Arepalli, S.; Tour, J. M.; Krishnamoorti, R. Macromolecules 2002, 35, 8825.
32. Thakre, P. R.; Lagoudas, D. C.; Zhu, J.; Barrera, E. V.; Gates, T. S. Effect of Functionalization and Weight Fraction of Single Walled Carbon Nanotubes on Mechanical Properties of Epoxy Nanocomposites; International Conference on Computational and Experimental Engineering Sciences (ICCES-05): Chennai, India, 2005.
33. Zhu, J.; Kim, J. D.; Peng, H. Q.; Margrave, J. L.; Khabashesku, V. N.; Barrera, E. V. Nano Lett 2003, 3, 1107.
34. Zhu, J.; Peng, H. Q.; Rodriguez, M.; Margrave, J. L.; Khabasheskhu, V. N.; Imam, A. M.; Lozano, K.; Barrera, E. V. Adv Funct Mater 2004, 14, 643.
35. Yuen, S. M.; Ma, C. C. M.; Wu, H. H.; Kuan, H. C.; Chen, W. J.; Liao, S. H.; Hsu, C. W.; Wu, H. L. J Appl Polym Sci 2007, 103, 1272.
36. Winey, K. I.; Kashiwagi, T.; Mu, M. F. MRS Bull 2007, 32, 348.
37. Ma, P. C.; Kim, J. K.; Tang, B. Z. Compos Sci Technol 2007, 67, 2965.
38. Li, C. Y.; Thostenson, E. T.; Chou, T. W. Appl Phys Lett 2007, 91, 223114-1.
39. Gao, L.; Zhou, X. F.; Ding, Y. L. Chem Phys Lett 2007, 434, 297.
40. Bal, S.; Samal, S. S. Bull Mater Sci 2007, 30, 379.
41. Schulte, K.; Gojny, F. H.; Wichmann, M. H. G.; Sumfleth, J.; Fiedler, B. Materialwissenschaft Und Werkstofftechnik 2006, 37, 698.
42. Song, Y. S.; Youn, J. R. Carbon 2005, 43, 1378.
43. Kim, Y. J.; Shin, T. S.; Choi, H. D.; Kwon, J. H.; Chung, Y. C.; Yoon, H. G. Carbon 2005, 43, 23.
44. Barrau, S.; Demont, P.; Maraval, C.; Bernes, A.; Lacabanne, C. Macromol Rapid Commun 2005, 26, 390.
45. Kim, B.; Lee, J.; Yu, I. S. J Appl Phys 2003, 94, 6724.
46. Allaoui, A.; Bai, S.; Cheng, H. M.; Bai, J. B. Compos Sci Technol 2002, 62, 1993.
47. Available at: http://www.cnanotech.com/products/materials.html.
48. Tao, K.; Yang, S. Y.; Grunlan, J. C.; Kim, Y. S.; Dang, B. L.; Deng, Y. J.; Thomas, R. L.; Wilson, B. L.; Wei, X. J Appl Polym Sci 2006, 102, 5248.
49. Bekyarova, E.; Thostenson, E. T.; Yu, A.; Itkis, M. E.; Fakhrutdinov, D.; Chou, T. W.; Haddon, R. C. J Phys Chem C 2007, 111, 17865.
50. Grujicic, M.; Cao, G.; Roy, W. N. J Mater Sci 2004, 39, 4441.
51. Ounaies, Z.; Park, C.; Wise, K. E.; Siochi, E. J.; Harrison, J. S. Compos Sci Technol 2003, 63, 1637.